Azimuthal entanglement and multichannel Schmidt-type decomposition of noncollinear biphotons

M. V. Fedorov*

A.M. Prokhorov General Physics Institute, Russian Academy of Sciences, 38 Vavilov st., Moscow, 119991, Russia
and National Research Nuclear University MEPhI (Moscow Engineering Physics Institute), 31 Kashirskoe Shosse, Moscow 115409, Russia

(Received 3 January 2016; revised manuscript received 8 February 2016; published 15 March 2016)

Purely azimuthal entanglement is analyzed for noncollinear frequency-degenerate biphoton states. The degree of azimuthal entanglement is found to be very high, with the Schmidt parameter K on the order of the ratio of the pump waist to its wavelength. A scheme is suggested for partial realization of this high entanglement resource in the form of a multichannel Schmidt-type decomposition.

DOI: 10.1103/PhysRevA.93.033830

I. INTRODUCTION

A structure of emission in the type-I noncollinear spontaneous parametric down-conversion (SPDC) is well known: SPDC photons propagate along a cone with the axis $(0z)$ coinciding with the central propagation direction of the pump, and section of the cone by the plane $(xy) \perp 0z$ is a ring [1–3]. As quantum objects, SPDC photons are characterized by their wave function depending on transverse components of wave vectors $\vec{k}_{1\perp}$ and $\vec{k}_{2\perp}$, where the indices 1 and 2 indicate two indistinguishable SPDC photons and $\perp$ refers to the plane (xy). Each of two SPDC photons has two degrees of freedom; for example, corresponding to motions in $0x$ and $0y$ directions. In this specific case the biphoton wave function depends on two pairs of variables, $k_{1,2x}$ and $k_{1,2y}$. Alternatively, the wave vectors $\vec{k}_{1,2\perp}$ can be characterized by their absolute values $\rho_{1,2} = |\vec{k}_{1,2\perp}|$ and angles with respect to the x axis (azimuthal angles), $\alpha_{1,2}$. This parametrization of transverse wave vectors $\vec{k}_{1,2\perp}$ is widely used in the analysis based on the concept of the orbital angular momentum (OAM) of photons [4–7]. Parametrization used in the present work slightly differs from that used in the OAM analysis. The transverse wave vectors $\vec{k}_{1,2\perp}$ are assumed to be characterized by spherical angles of the total wave vectors $\vec{k}_i$, i.e., by polar (zenith) angles $\theta_{1,2}$ defined as angles between $\vec{k}_i$ and the z axis, and azimuthal angles $\alpha_{1,2}$ defined, as previously, as angles between $\vec{k}_{i\perp}$ and the x axis. In terms of these definitions one can investigate separately entanglement of noncollinear biphotons either in polar or in azimuthal angular variables. As far as I know, this formulation of the problem differs from that used in the OAM analysis where azimuthal and "radial" entanglements (in variables $\alpha_{1,2}$ and $\rho_{1,2}$) are considered usually as inseparable parts of the total biphoton entanglement. As argued below, consideration of azimuthal entanglement itself has sense both for theoretical analysis and, potentially, for practical experimental researches and applications. For the cases of sufficiently pronounced degree of noncollinearity, the degree of azimuthal entanglement will be shown to be very high and, roughly, determined by a large parameter of the pump waist divided by its wavelength. In principle, this provides a very large resource of azimuthal entanglement, and a scheme for its partial realization in experiments will be described.

*fedorovmv@gmail.com

II. BIPHOTON ANGULAR WAVE FUNCTION

A. General expressions

Let us consider a biphoton state formed in the noncollinear frequency-degenerate process of spontaneous parametric down-conversion (SPDC) with a cw pump and with phase matching of type I. In this case the pump is propagating in a nonlinear crystal as the extraordinary wave, and some photons of the pump decay for two indistinguishable photons "1" and "2" of the ordinary wave, $e \to o + o$. The emitted photons are assumed to have coinciding frequencies equal to the half of a given frequency of the pump, $\omega_1 = \omega_2 = \omega_p/2$, and coinciding horizontal polarizations. Let the pump be propagating along the z axis and having the waist w. As usual, the pump waist w is assumed to be much smaller than the transverse sizes of a crystal, which provides the transverse-momentum conservation rule:

$$\vec{k}_{p\perp} = \vec{k}_{1\perp} + \vec{k}_{2\perp}, \tag{1}$$

where $\vec{k}_{p\perp}$ is the projection of the pump wave vector $\vec{k}_p$ on the plane (xy) perpendicular to the z axis. In the transverse-momentum representation the wave function of two emitted photons is known to have the form [8–10]

$$\Psi \propto \exp\left[-\frac{w_p^2}{2}(\vec{k}_{1\perp} + \vec{k}_{2\perp})^2\right] \mathrm{sinc}\left(\frac{L\Delta}{2}\right), \tag{2}$$

where the pump amplitude is taken to be Gaussian with the waist w_p, $\mathrm{sinc}(x) = \sin x/x$, and L is the length of a crystal in the pump-propagation direction; Δ is the phase mismatch

$$\Delta = k_{pz} - k_{1z} - k_{2z} \approx \Delta_0 + \frac{(\vec{k}_{1\perp} - \vec{k}_{2\perp})^2}{4k_1} \tag{3}$$

and

$$\Delta_0 = k_p - k_1 - k_2. \tag{4}$$

The wave function (2) is assumed to obey the unit normalization condition $\int d\vec{k}_{1\perp} d\vec{k}_{2\perp} |\Psi|^2 = 1$. The proportionality symbol is used in Eq. (2) and below instead of writing down explicitly the normalization constant (to avoid too cumbersome formulas).

B. Spherical angles

In accordance with the goals declared in the Introduction, let us characterize orientation of wave vectors in a free space

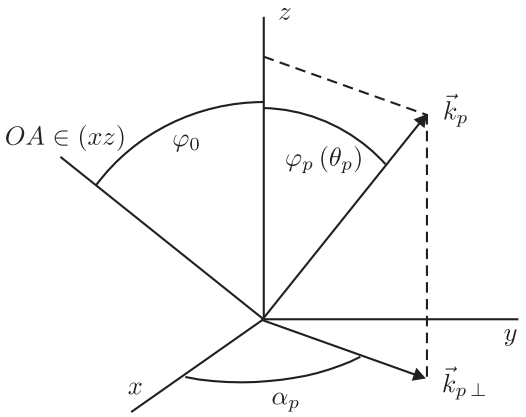

FIG. 1. Azimuthal (α_p) and polar [$\varphi_p(\theta_p)$] angles of the wave vector $\vec{k}_p$ (φ_p inside and θ_p outside the crystal); φ_0 is the angle between the crystal's major optical axis OA and the central propagation direction of the pump (the z axis).

after the crystal by their spherical angles—polar angles $\theta_{p,1,2}$ and azimuthal angles $\alpha_{p,1,2}$:

$$\begin{aligned}\vec{k}_p &= \frac{2\pi}{\lambda_p}\{\sin\theta_p\cos\alpha_p,\ \sin\theta_p\sin\alpha_p,\ \cos\theta_p\},\\ \vec{k}_1 &= \frac{\pi}{\lambda_p}\{\sin\theta_1\cos\alpha_1,\ \sin\theta_1\sin\alpha_1,\ \cos\theta_1\},\\ \vec{k}_2 &= -\frac{\pi}{\lambda_p}\{\sin\theta_2\cos\alpha_2,\ \sin\theta_2\sin\alpha_2,\ \cos\theta_2\},\end{aligned} \tag{5}$$

where λ_p is the pump wavelength. As an example, the polar and azimuthal angles of the pump wave vector are shown in Fig. 1, with the coordinate frame turned intentionally for clearer visibility in such a way that the z axis is vertical, though traditionally and in all further illustrations the propagation axis $0z$ is taken to be horizontal. Two different notations, φ_p and θ_p, are used for polar angles of $\vec{k}_p$ inside and outside a crystal. Similar pairs of notations are used below for polar angles of SPDC photons $\vec{k}_{1,2}$: $\varphi_{1,2}$ and $\theta_{1,2}$.

The sign "$-$" in the definition of $\vec{k}_2$ in Eq. (5) deserves a special explanation. It is known [1–3] that in the noncollinear SPDC process two photons of each pair are located approximately at the opposite ends of diameters of the ring formed by a section of the emission cone by the transverse plane $(xy)\perp 0z$. This condition is provided in different ways in the two-dimensional (2D) and three-dimesional (3D) geometries. In the plane geometry, deviations from the z axis can be characterized by angles $\theta_{1,2}$ having different signs for "up" and "down" (or "left" and "right") deviations [11]. In contrast, in the 3D geometry, both polar angles θ_1 and θ_2 are always positive ($\pi \geqslant \theta_{1,2} \geqslant 0$). In this case the condition of location at the opposite ends of the ring diameters is provided by different definitions of the azimuthal angles of two photons: these angles have to differ from each other approximately by the term π. Alternatively, it is possible to define azimuthal angles α_1 and α_2 as being close to each other but counted from different directions of the x axis: the angle α_1 counted from the positive direction of the x axis and the angle α_2 counted from its negative direction. This definition is illustrated by Fig. 2,

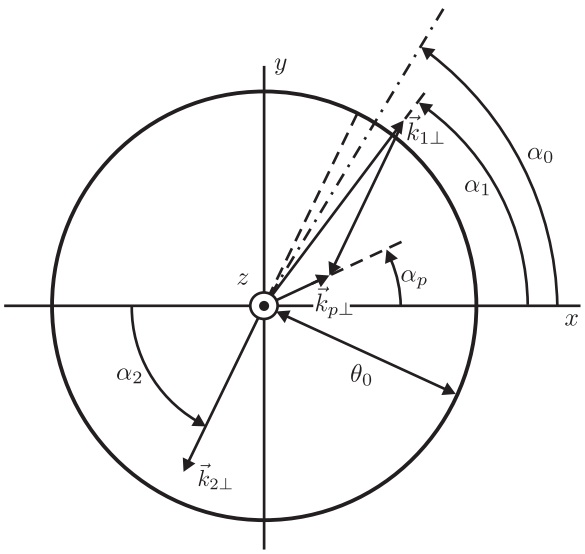

FIG. 2. Section of the emission cone by the plane $(xy)\perp 0z$: α_1 and α_2 are the azimuthal angles of emitted photons, $\alpha_0 = \frac{1}{2}(\alpha_1+\alpha_2)$, and θ_0 is the opening angle of the cone.

which shows schematically the orientation of transverse wave vectors $\vec{k}_{1\perp}$ and $\vec{k}_{2\perp}$, as well as their azimuthal angles α_1 and α_2. The inset in Fig. 2 is a diagram of the transverse-momentum conservation rule (1). It is worth noting that only two vectors of this diagram, $\vec{k}_{1\perp}$ and $\vec{k}_{2\perp}$, are controllable experimentally by positions of detectors, whereas the transverse component of the pump wave vector, $\vec{k}_{p\perp}$, is selected automatically from all of its possible values and directions by the conservation rule (1).

Representation of wave vectors in terms of spherical angles (5) can be used to find rather simple expressions for the squared difference and sum of $\vec{k}_{1\perp}$ and $\vec{k}_{2\perp}$ in Eq. (3):

$$\begin{aligned}|\vec{k}_{1\perp}\pm\vec{k}_{2\perp}|^2 = \frac{\pi^2}{\lambda_p^2}[&\sin^2\theta_1+\sin^2\theta_2\\ &\mp 2\sin\theta_1\sin\theta_2\cos(\alpha_1-\alpha_2)].\end{aligned} \tag{6}$$

Let us assume now that deviations of wave vectors $\vec{k}_1$ and $\vec{k}_2$ from the z axis, as well as the difference of their azimuthal angles, are small. Let also deviations of the polar angles $\theta_{1,2}$ from the cone-opening angle θ_0 be much smaller than θ_0; i.e., the thickness of the ring in Fig. 2 be much smaller than its radius. Mathematically these assumptions are formulated as

$$|\theta_{1,2}-\theta_0| \ll \theta_0 \ll 1, \quad |\alpha_1-\alpha_2| \ll 1. \tag{7}$$

In these approximations Eq. (6) takes the much simpler form

$$|\vec{k}_{1\perp}\pm\vec{k}_{2\perp}|^2 \approx \frac{\pi^2}{\lambda_p^2}\left[(\theta_1\mp\theta_2)^2+\theta_0^2(\alpha_1-\alpha_2)^2\right]. \tag{8}$$

C. Refractive index of the pump wave

In a crystal, absolute values of the wave vectors k_p and $k_{1,2}$ are determined by the corresponding refractive indices: $k_1 = k_2 = \frac{\pi}{\lambda_p}n_o(2\lambda_p)$ and $k_p = \frac{2\pi}{\lambda_p}n_p(\lambda_p,\varphi_0,\alpha_p,\varphi_p)$, where $n_o(\lambda)$ is the isotropic refractive index of the ordinary wave depending only on the light wavelength, and the pump

refractive index is given by

$$n_p(\lambda_p,\varphi_p,\alpha_p,\varphi_0) = n_o(\lambda_p)n_e(\lambda_p)\{n_o^2(\lambda_p)[\sin^2\varphi_p\sin^2\alpha_p + (\sin\varphi_p\cos\varphi_0\cos\alpha_p + \cos\varphi_p\sin\varphi_0)^2] + n_e^2(\lambda_p)(\cos\varphi_p\cos\varphi_0 - \sin\varphi_p\sin\varphi_0\cos\alpha_p)^2\}^{-1/2}. \quad (9)$$

In this formula $n_e(\lambda_p)$ is the extraordinary-wave refractive index for the propagation direction along the minor axis of the polarization ellipse of a crystal. The functions $n_o(\lambda_p)$ and $n_e(\lambda_p)$ are determined by the well-known Sellmeier formulas [12]. For a β-BaB_2O_4 (BBO) crystal at $\lambda_p = 0.4047\ \mu$m [13] the numerical values of these functions are $n_o(0.4047\ \mu\text{m}) = 1.69236$ and $n_e(0.4047\ \mu\text{m}) = 1.56801$.

Note that Eq. (9) can be written in a standard and familiar form [14],

$$n(\vartheta) = \frac{n_o(\lambda_p)n_e(\lambda_p)}{[n_o(\lambda_p)^2\sin^2\vartheta + n_e(\lambda_p)^2\sin^2\vartheta\cos^2\vartheta]^{1/2}} \quad (10)$$

with ϑ being the angle between $\vec{k}_p$ and the crystal optical axis. Equation (10) turns into (9) when ϑ is expressed in terms of the angles φ_p, α_p, and φ_0 of Fig. 1.

As all deviations from the z axis are assumed to be small, the refractive index of Eq. (9) can be expanded in powers of φ_p. With only two first terms of this expansion retained, the term Δ_0 (4) in Eq. (3) takes the form

$$\Delta_0 = \frac{2\pi}{\lambda_p}[n_p(\lambda_p,\varphi_p,\alpha_p,\varphi_0) - n_o(2\lambda_p)] \approx \frac{2\pi}{\lambda_p}[n_p(\varphi_0) - n_o + n_p'(\lambda_p,\alpha_p,\varphi_0)\varphi_p], \quad (11)$$

where $n_p(\varphi_0) \equiv n_p(\lambda_p,0,0,\varphi_0)$ and $n_o = n_o(2\lambda_p) = 1.66109\ \mu$m.

The derivative of the refractive index is defined as

$$n_p'(\lambda_p,\alpha_p,\varphi_0) = \left.\frac{\partial n_p(\lambda_p,\varphi_p,\alpha_p,\varphi_0)}{\partial\varphi_p}\right|_{\varphi_p=0}. \quad (12)$$

A sufficiently simple expression for n_p' can be found analytically by a direct differentiation of the expression in Eq. (9):

$$n_p'(\lambda_p,\alpha_p,\varphi_0) = -\zeta(\lambda_p,\varphi_0)\cos\alpha_p, \quad (13)$$

with the coefficient $\zeta(\lambda_p,\varphi_0)$ having the form

$$\zeta(\lambda_p,\varphi_0) = \frac{n_o(\lambda_p)n_e(\lambda_p)[n_o^2(\lambda_p) - n_e^2(\lambda_p)]\sin\varphi_0\cos\varphi_0}{[n_o^2(\lambda_p)\sin^2\varphi_0 + n_e^2(\lambda_p)\cos^2\varphi_0]^{3/2}}. \quad (14)$$

The term with the derivative of the refractive index n_p' in Eq. (11) determines the well-known spatial walk-off effects. Very often this term is omitted from consideration at all. Let us refer this simplification as corresponding to the 'no walk-off" or NWO approximation. As shown below, for azimuthal entanglement, in the case of sufficiently well pronounced noncollinearity, the NWO approximation is reasonably good. But in a general case the walk-off term can be important because it takes into account anisotropy of birefringent crystals and breaks the axial symmetry of the SPDC process [10] occurring in the NWO approximation. As follows from the cosine dependence of n_p' (13) on α_p, the walk-off effects are maximal in the cases $\alpha_p = 0$ or π, i.e., when the pump wave vector $\vec{k}_p$ belongs to the plane (OA,z) formed by the crystal optical axis and the central propagation direction of the pump. Oppositely, the walk-off term vanishes in the case $\alpha_p = \pi/2$ when the pump wave vector is located in the plane (y,z) perpendicular to the optical-axis plane (OA,z).

A structure and the role of the walk-off term will be discussed in more details in Sec. II E. But before this, let us discuss the structure of other terms in the phase mismatch of Eq. (3).

D. The NWO parts of the phase mismatch, linear approximation

The term $n_p(\varphi_0) - n_o$ in Eq. (11) determines the dependence of the phase mismatch on the angle φ_0 between the optical axis and the central pump propagation direction $0z$. For a BBO crystal and the pump wavelength $\lambda_p = 0.4047\ \mu$m this dependence is shown in Fig. 3. The angle $\varphi_0^{\text{coll}} = 0.5$ corresponds to the collinear SPDC regime, and the noncollinear regime occurs at $0.5 < |\varphi_0| < 2.64$. In further numerical examples the angle φ_0 will be taken to be equal to 0.7 rad. In particular, at these parameters the numerical value of the coefficient ζ (14) in the derivative of the refractive index (13) equals $\zeta(0.4047\ \mu\text{m}, 0.7) \approx 0.12$.

The second NWO part in the phase mismatch (3), $\frac{1}{4k_1}(\vec{k}_{1\perp} - \vec{k}_{2\perp})^2$, is determined by Eq. (8), and together with the expression of Eq. (11) this gives

$$\Delta_{\text{NWO}} = \pi\frac{(\theta_1+\theta_2)^2 + 8n_o(n_p - n_o) - \theta_0^2(\alpha_1-\alpha_2)^2}{4n_o\lambda_p} \equiv \frac{\pi}{4n_o\lambda_p}[(\theta_1+\theta_2)^2 - 4\theta_0^2 - \theta_0^2(\alpha_1-\alpha_2)^2], \quad (15)$$

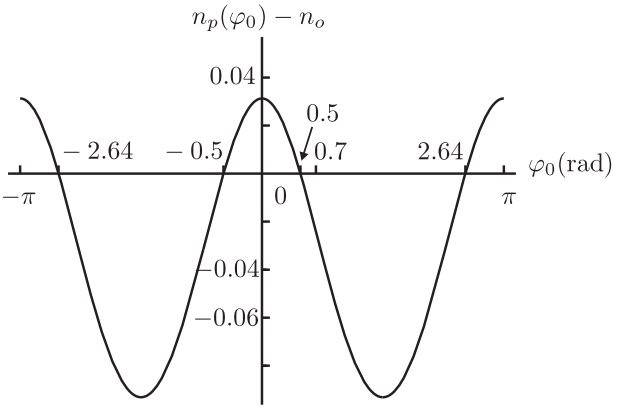

FIG. 3. The difference of the refractive indices $n_p - n_o$ as a function of φ_0 for a BBO crystal and the wavelength $\lambda_p = 0.4047\ \mu$m.

where the angular width of the emission cone θ_0 is defined at last as

$$\theta_0 = \sqrt{2n_o(n_o - n_p)}. \tag{16}$$

Numerically, for a BBO crystal at $\lambda_p = 0.4047\ \mu$m and $\varphi_0 = 0.7$, Eq. (16) yields $\theta_0 = 0.28 \approx 16^\circ$.

The next simplification step is the linear approximation in the phase mismatch similar to that of Ref. [11]. The $\theta_{1,2}$-dependent part of the expression in square brackets in the second line of Eq. (15) can be rewritten as

$$(\theta_1 + \theta_2)^2 - 4\theta_0^2 \equiv 4\theta_0(\theta_1 + \theta_2 - 2\theta_0) + (\theta_1 + \theta_2 - 2\theta_0)^2. \tag{17}$$

Owing to the assumptions of Eq. (7), the second, quadratic, term on the right-hand side of this equation is much smaller than the first, linear term, $\theta_1 + \theta_2 - 2\theta_0$. In the linear approximation the quadratic terms in $\theta_{1,2} - \theta_0$ can be dropped, as well as the term quadratic in the difference of azimuthal angles in Eq. (15), $\theta_0^2(\alpha_1 - \alpha_2)^2$, to give

$$\Delta_{\mathrm{NWO}}^{\mathrm{lin}} = \frac{\pi}{n_o\lambda_p}\theta_0(\theta_1 + \theta_2 - 2\theta_0). \tag{18}$$

Smallness of contributions of the dropped quadratic terms to the argument of the sinc function will be estimated below in Sec. II F.

Note also that, in accordance with Eq. (15), the constant part of the phase mismatch, which is independent of any variables, equals $-\pi\theta_0^2/n_o\lambda_p$, and this gives the following expression for the constant term in the argument of the sinc function in Eq. (2):

$$\phi = \left.\frac{L\Delta_0}{2}\right|_{\theta_{1,2}=0,\alpha_1=\alpha_2} = -\frac{\pi\theta_0^2 L}{2n_o\lambda_p}. \tag{19}$$

Estimated at the same values of parameters as indicated above ($\theta_0 = 0.28$, $\lambda_p = 0.4047\ \mu$m, $n_o = 1.66109\ \mu$m) and $L = 0.5$ cm, Eq. (19) gives $\phi \approx -925$, which exceeds significantly the values $\phi = -2.3$ or $\phi = -4$ of Refs. [7] and [6]. At the same values of λ_p, L and n_o as used above, the indicated small values of ϕ correspond to a very small degree of noncollinearity, $\theta_0 \leqslant 0.019 \approx 1^\circ$. As shown below, this large difference with the case under consideration ($\theta_0 = 0.28 \approx 16^\circ$) explains a large difference in the predicted degree of azimuthal entanglement.

E. Evaluation of the "walk-off" term

Let us consider now the "walk-off" term in the phase mismatch determined by Eqs. (11) and (13):

$$\Delta_0^{\mathrm{WO}} = -\frac{2\pi}{\lambda_p}\zeta(\lambda_p,\varphi_0)\varphi_p\cos\alpha_p. \tag{20}$$

In this formula φ_p is the polar angle of the pump wave vector inside the crystal and α_p is its azimuthal angle, uncontrollable directly in experiments. Both of them have to be expressed in terms of the experimentally controllable photon angles $\theta_{1,2}$ and $\alpha_{1,2}$ in free space after the crystal. This can be done with the help of Eq. (1) (the transverse-momentum conservation rule).

At first, note that the tangent components of wave vectors are continuous at the crystal-vacuum boundary. For this reason the left- and right-hand sides of Eq. (1) can be evaluated, correspondingly, inside and outside the crystal to give, for the squared terms on both sides of this equation,

$$k_p^2\sin^2\varphi_p \approx k_p^2\varphi_p^2 = (\vec{k}_{1\perp} + \vec{k}_{2\perp})^2 \tag{21}$$

or

$$\varphi_p = \frac{\lambda_p}{2\pi n_p}|\vec{k}_{1\perp} + \vec{k}_{2\perp}|, \tag{22}$$

with known expressions for $(\vec{k}_{1\perp} + \vec{k}_{2\perp})^2$ and, hence, $|\vec{k}_{1\perp} + \vec{k}_{2\perp}|$ in terms of $\theta_{1,2}$ and $\alpha_{1,2}$ [(6) and (8)].

Another way of using Eq. (1) consists of projecting both of its sides on the direction perpendicular to the vector $\vec{k}_{p\perp}$. Then, clearly, the left-hand side of Eq. (1) gives zero, and the right-hand side gives the equation for finding $\cos\alpha_p$:

$$\sin\theta_1\sin(\alpha_1 - \alpha_p) - \sin\theta_2\sin(\alpha_2 - \alpha_p) = 0, \tag{23}$$

The solution of this equation is given by

$$\cos\alpha_p = \frac{\sin\theta_1\cos\alpha_1 - \sin\theta_2\cos\alpha_2}{[\sin^2\theta_1 + \sin^2\theta_2 - 2\sin\theta_1\sin\theta_2\cos(\alpha_1 - \alpha_2)]^{1/2}}. \tag{24}$$

The denominator of this expression is easily recognized to be coinciding with the angular part of $|\vec{k}_{1\perp} - \vec{k}_{2\perp}|$ of Eq. (6). The numerator of the fraction in Eq. (24), as previously done, can be expanded in powers $|\theta_1 - \theta_2|$ and $|\alpha_1 - \alpha_2|$ with only the lowest-order (linear) terms being retained. Then the final expression for $\cos\alpha_p$ takes the form

$$\cos\alpha_p = \frac{\pi/\lambda_p}{|\vec{k}_{1\perp} + \vec{k}_{2\perp}|} \times [(\theta_1 - \theta_2)\cos\alpha_0 - \theta_0\sin\alpha_0(\alpha_1 - \alpha_2)], \tag{25}$$

where

$$\alpha_0 = \frac{\alpha_1 + \alpha_2}{2}. \tag{26}$$

In contrast to the difference of azimuthal angles $\alpha_1 - \alpha_2$, which is assumed to be small, their sum and a half-sum α_0 can change in rather wide ranges, $\frac{\pi}{2} \geqslant \alpha_0 \geqslant -\frac{\pi}{2}$. With the obtained expressions (22) and (25), the contribution (20) of the walk-off term into the phase mismatch Δ takes the form

$$\Delta_0^{\mathrm{WO}} = -\pi\zeta\frac{(\theta_1 - \theta_2)\cos\alpha_0 - \theta_0\sin\alpha_0(\alpha_1 - \alpha_2)}{\lambda_p n_p}. \tag{27}$$

Note that this expression can seem to be antisymmetric with respect to the variable transposition $\theta_1 \rightleftharpoons \theta_2$, $\alpha_1 \rightleftharpoons \alpha_2$, which cannot be true. However, it should be kept in mind that, in accordance with the definition of the angles $\alpha_{1,2}$ shown in Fig. 2, the variable transposition must be accompanied by the shift of both angles α_1 and α_2 for π, which changes the signs of $\cos\alpha_0$ and $\sin\alpha_0$ and provides the symmetry of the expression (27).

F. Final expressions for the wave function and its double-Gaussian representation

Summation of all derived results (2), (18), and (27) gives the following general expression for the biphoton angular wave

function:

$$\Psi \propto \exp\left\{-\frac{(\theta_1-\theta_2)^2+\theta_0^2(\alpha_1-\alpha_2)^2}{2\Delta\theta_p^2}\right\} \times \mathrm{sinc}\left\{\frac{1}{2\Delta\theta_L}\left[\theta_0(\theta_1+\theta_2-2\theta_0) - \frac{n_o}{n_p}\zeta(\cos\alpha_0(\theta_1-\theta_2)-\sin\alpha_0\theta_0(\alpha_1-\alpha_2))\right]\right\}, \quad (28)$$

where $\Delta\theta_p = \lambda_p/\pi w_p$ and $\Delta\theta_L = n_o\lambda_p/\pi L$, and the first exponential factor is the pump angular amplitude of Eq. (2) with the expression for $(\vec{k}_{1\perp}+\vec{k}_{2\perp})^2$ taken from Eq. (8).

As mentioned above, in principle, the walk-off terms make the angular biphoton wave function axially asymmetric, which is seen in its dependence not only on the difference of azimuthal angles $\alpha_1-\alpha_2$ but also on their sum via α_0 (26). The symmetry returns in the NWO approximation when the expression (28) takes the form

$$\Psi_{\mathrm{NWO}} \propto \exp\left\{-\frac{(\theta_1-\theta_2)^2+\theta_0^2(\alpha_1-\alpha_2)^2}{2\Delta\theta_p^2}\right\} \times \mathrm{sinc}\left\{\frac{1}{2\Delta\theta_L}[\theta_0(\theta_1+\theta_2-2\theta_0)]\right\}. \quad (29)$$

In addition to the dependence only on the difference of azimuthal angles $\alpha_1-\alpha_2$, the remarkable feature of the NWO approximation consists of factorization of the dependencies on polar and azimuthal angles. In other words, the NWO wave function (29) takes the form of a product of two factors $\Psi_{\mathrm{NWO}} = \Psi^{\mathrm{pol}}_{\mathrm{NWO}} \times \Psi^{\mathrm{az}}_{\mathrm{NWO}}$, with $\Psi^{\mathrm{pol}}_{\mathrm{NWO}}$ and $\Psi^{\mathrm{az}}_{\mathrm{NWO}}$ depending, correspondingly, only on polar and only on azimuthal angles:

$$\Psi^{\mathrm{pol}}_{\mathrm{NWO}}(\theta_1,\theta_2) \propto \exp\left\{-\frac{(\theta_1-\theta_2)^2}{2\Delta\theta_p^2}\right\} \times \mathrm{sinc}\left\{\frac{1}{2\Delta\theta_L}[\theta_0(\theta_1+\theta_2-2\theta_0)]\right\} \quad (30)$$

and

$$\Psi^{\mathrm{az}}_{\mathrm{NWO}}(\alpha_1,\alpha_2) \propto \exp\left\{-\frac{\theta_0^2(\alpha_1-\alpha_2)^2}{2\Delta\theta_p^2}\right\}. \quad (31)$$

These simple expressions for the polar and azimuthal wave functions can be used for explicit evaluation of smallness of contributions to the argument of the sinc function from the dropped quadratic terms in the transition from Eq. (15) to Eq. (18). Indeed, in accordance with Eq. (30), a characteristic value of $\theta_1+\theta_2-2\theta_0$ can be found from the condition that the argument of the sinc function is on the order of unity, which gives $\theta_1+\theta_2-2\theta_0 \sim \Delta\theta_L/\theta_0$. Then the contribution to the argument of the sinc function from the dropped quadratic term in the phase mismatch (17) is evaluated as

$$\frac{(\theta_1+\theta_2-2\theta_0)^2}{\Delta\theta_L} \sim \frac{\Delta\theta_L}{\theta_0} \sim \frac{\lambda_p}{\theta_0^2 L} \sim 10^{-3} \ll 1, \quad (32)$$

for $L = 0.5$ cm, $\lambda_p \sim 0.5$ μm, and $\theta_0^2 \sim 0.1$.

The second dropped quadratic term in the linearized phase mismatch (18) is $\theta_0^2(\alpha_1-\alpha_2)^2$. The difference of azimuthal angles can be estimated from Eq. (31) as $|\alpha_1-\alpha_2| \sim \Delta\theta_p/\theta_0$, and this gives the following estimate for its contribution to the argument of the sinc function:

$$\frac{\theta_0^2(\alpha_1-\alpha_2)^2}{\Delta\theta_L} \sim \frac{\Delta\theta_p^2}{\Delta\theta_L} \sim \frac{L\lambda_p}{w_p^2} \sim 10^{-4} \ll 1 \quad (33)$$

at $w_p = L = 0.5$ cm and $\lambda_p \sim 0.5$ μm. Actually, the expression on the right-hand side of the last equation is the inverse Rayleigh range or the ratio of the crystal length to the diffraction length of the pump. In any case, the estimates of Eqs. (32) and (33) indicate clearly that at the chosen values of all parameters the linear approximation of the phase mismatch (18) is perfectly justified.

In contrast to the considered case, beyond the NWO approximation, with the walk-off terms taken into account, there is no factorization in the wave function of Eq. (28) for parts depending on polar and azimuthal variables, and no axial symmetry. However, the linear approximation for the phase mismatch remains valid.

The next step of simplifications in the general expression (28) consists of the replacement of the squared sinc function by the appropriately chosen Gaussian function [15–17]. For the case with the argument of the sinc function being a linear function of variables, the best modeling is

$$\mathrm{sinc}^2(x) \to \exp(-0.359x^2), \quad (34)$$

with 0.359 being the best fitting parameter. With this replacement, Eq. (28) takes the form

$$|\Psi(\theta_1,\alpha_1;\theta_2,\alpha_2)|^2 \propto \exp\left[-\frac{(\theta_1-\theta_2)^2+\theta_0^2(\alpha_1-\alpha_2)^2}{\Delta\theta_p^2}\right] \times \exp\left\{-\frac{0.359}{4\Delta\theta_L^2}\left[\theta_0(\theta_1+\theta_2-2\theta_0) - \frac{n_o}{n_p}\zeta(\cos\alpha_0(\theta_1-\theta_2)-\sin\alpha_0\theta_0(\alpha_1-\alpha_2))\right]^2\right\}. \quad (35)$$

Note that the arguments of both exponents are quadratic in variables and, thus, the linear approximation in the argument of the sinc function in Eq. (28) fits perfectly the quadratic dependencies in the Gaussian functions (35).

The expression (35) for the squared biphpoton azimuthal-polar wave function can be integrated over either polar or azimuthal angles to give, correspondingly, purely azimuthal or purely polar probability density distributions. The polar distribution received in this way looks rather complicated and will be analyzed and discussed elsewhere, whereas the azimuthal distribution is discussed in detail in the following section.

III. ENTANGLEMENT

As mentioned in the Introduction, the main goal of the present consideration consists of characterization and evaluation of the purely azimuthal entanglement of biphotons independently of entanglement in the second degree of freedom, i.e., in polar angles.

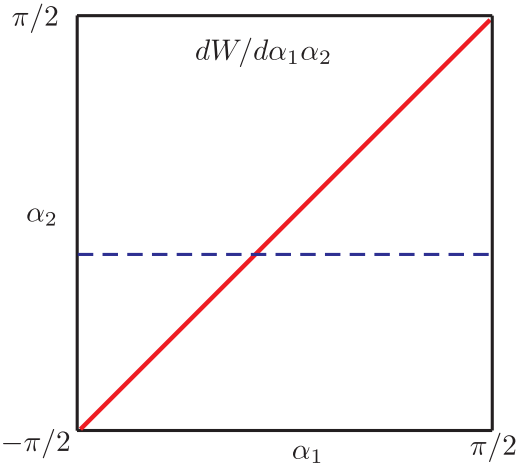

FIG. 4. Density plot of the biphoton azimuthal distribution (36).

A. Coincidence and single-particle widths

It is known [18,19] that the degree of entanglement of bipartite states with continuous variables can be found by means of single-particle and coincidence measurements. Such measurements can be used to plot curves of the corresponding distributions of numbers of registered particles in dependence on the corresponding variables. The ratio of widths of the single-particle and coincidence distributions is the parameter R characterizing the degree of entanglement [18]. Mathematically, this parameter is defined as the ratio of the widths of the curves of unconditional and conditional probability densities. For double-Gaussian wave functions this parameter is known [19] to coincide exactly with the Schmidt parameter $K = 1/Tr(\rho_r^2)$, where ρ_r is the reduced density matrix of the bipartite state. It is clear also that if particles in a bipartite state have two degrees of freedom, then to find probability distributions and entanglement in one of these degrees of freedom, one has to integrate the total two-degrees-of-freedom distribution over variables characterizing the second degree of freedom.

Complete independence of azimuthal and polar-angle parts in the biphoton angular wave function occurs in the NWO approximation (29), when the distribution of the biphoton azimuthal probability density is given by

$$\frac{dW^{\rm az}_{\rm NWO}}{d\alpha_1 d\alpha_2} = \left|\Psi^{\rm az}_{\rm NWO}\right|^2 = \frac{\Delta\theta_p/\theta_0}{\pi^{3/2}} \exp\left[-\frac{\theta_0^2(\alpha_1-\alpha_2)^2}{\Delta\theta_p^2}\right], \tag{36}$$

with $|\alpha_{1,2}| \leqslant \pi/2$ and

$$\frac{\pi}{2} \geqslant \alpha_0 \equiv \frac{\alpha_1+\alpha_2}{2} \geqslant -\frac{\pi}{2}. \tag{37}$$

As $\Delta\theta_p$ is very small ($\sim\lambda_p/w_p \sim 10^{-4}$), the preexponential coefficient in the expression on the right-hand side of equation (36) provides the unit normalization of the probability density,

$$\int d\alpha_1 d\alpha_2 \frac{dW^{\rm az}_{\rm NWO}}{d\alpha_1 d\alpha_2} = 1.$$

The density plot of the distribution (36) is shown schematically in Fig. 4. In the map (α_1,α_2), this is a very narrow ridge of a unit hight, going along the diagonal $\alpha_1 = \alpha_2$ from $\alpha_1 = \alpha_2 = -\pi/2$ and up to $\alpha_1 = \alpha_2 = \pi/2$.

The coincidence distribution in α_1 has to be measured with two detectors: one of them counting photons only at some given value of α_2 and the second one scanning, in the map (α_1,α_2), along the horizontal line $\alpha_2 = $ const (the blue dashed line in Figure 4), and with only joint signals registered. In single-particle measurements one has to use only one detector scanning horizontally [in the map (α_1,α_2)] and registering all photons, independently of and at all possible values of the second-photon azimuthal angle α_2. Clearly, the coincidence and single-particle widths in such schemes of measurements are equal to

$$\Delta\alpha_1^{(c)} = \frac{\Delta\theta_p}{\theta_0}, \quad \Delta\alpha_1^{(s)} = \pi, \tag{38}$$

and they correspond to the entanglement parameter

$$R = \frac{\Delta\alpha_1^{(s)}}{\Delta\alpha_1^{(c)}} = \frac{\pi\theta_0}{\Delta\theta_p} = \pi^2\theta_0\frac{w_p}{\lambda_p} \sim 10^4. \tag{39}$$

Beyond the NWO approximation, polar and angular variables are not separated in the total wave function (28). In this case the bipartite azimuthal probability density can be obtained from the squared wave function of Eq. (35) by means of integration over the polar angles θ_1 and θ_2, or, equivalently, at first over $\theta_1+\theta_2$ and then over $\theta_1-\theta_2$. An important feature of this integration is related to the structure of the second exponential function in Eq. (35). Though it depends on both $\theta_1+\theta_2$ and $\theta_1-\theta_2$, its integration over $\theta_1+\theta_2$ from $-\infty$ to $+\infty$ gives just a number independent of any variables. This is a direct consequence of the linear approximation used for evaluation of the argument of the sinc function in Eq. (28). The second integration, over $\theta_1-\theta_2$, is carried out equally easy to give the expression for the azimuthal biphoton distribution coinciding with that derived in the NWO approximation (36) and shown in Fig. 4. Hence, all estimates of the azimuthal coincidence and single-particle widths (38), and of the parameter of azimuthal entanglement R (39) remain valid even beyond the NWO approximation when the walk-off term is taken into account in the phase mismatch in the linear approximation in $\theta_1 \pm \theta_2$ and $\alpha_1-\alpha_2$. Note that this proof is valid explicitly only for the described derivation of the parameter R, because the widths in its definition (39) are defined as widths of the probability distributions $dW/d\alpha_1 d\alpha_2|_{\alpha_2=\text{const}}$ and $\int d\alpha_2 dW/d\alpha_1 d\alpha_2$, rather than widths of wave functions. In contrast to this, the alternative derivations described in the following two subsections deal with wave functions and, thus, they are valid directly only in the NWO approximation.

Note also that the described picture of the biphoton distribution in azimuthal angular variables (36) is rather peculiar and unusual. Its very special feature is the dependence only on the difference of azimuthal angles of photons $\alpha_1-\alpha_2$ and the missing dependence on their sum or $\alpha_0 = \frac{1}{2}(\alpha_1+\alpha_2)$. In this case the only limitation for α_0 is related to its limited range of variation, $|\alpha_0| \leqslant \pi$. A great difference between this limitation and the width of the azimuthal distribution in $\alpha_1-\alpha_2$ ($\sim\Delta\theta_p/\theta_0$) is a factor providing a very high degree of azimuthal entanglement. These features of the azimuthal distri-

bution contrast with those of the above-mentioned distribution in polar angles $\theta_{1,2}$, as well as with features of distributions in Cartesian variables (e.g., $k_{x\,1,2}$ and $k_{y\,1,2}$), which are always characterized by wave functions with limited and comparable ranges of localization both in sums and differences of the corresponding variables. In this sense the azimuthal degree of freedom is unique: this is the only degree of freedom for which the distribution in variables has the above-described unusual features. Qualitatively there are two main reasons for such features of the biphoton azimuthal distribution. One of them is the axial symmetry of the biphoton distribution occurring in the NWO approximation. Mathematically, this symmetry shows itself just in the missing dependence of the biphoton azimuthal-angle probability density (36) on $\alpha_0 = \frac{1}{2}(\alpha_1 + \alpha_2)$ and its dependence only on $\alpha_1 - \alpha_2$. But, as shown above, the same results occur even beyond the NWO approximation if the phase mismatch [(18) and (27)] and the argument of the sinc function in Eq. (28) are taken in the linear approximation in the angular variables $\theta_{1,2} - \theta_0$ and $\alpha_1 - \alpha_2$. In this approximation, though the walk-off terms do affect the distribution in the polar angles, they do not affect the distribution in the azimuthal-angle variables. Thus, the linear approximation is the second key reason for the unusual features of the azimuthal distribution and very high degree of azimuthal entanglement. Validity of the linear approximation is justified by the assumption about sufficiently high noncollinearity of the SPDC process determined by the conditions (7). Transition to the case of smaller noncollinearity, and related modifications in the character and degree of azimuthal entanglement, will be discussed separately elsewhere.

B. Schmidt-mode analysis

The same results as described above can be obtained in the Schmidt-decomposition formalism. Azimuthal Schmidt modes can be found with the help of a slight modification in the azimuthal wave function $\Psi_{\rm NWO}$ (29). Let the restriction $|\alpha_0| \leqslant \pi/2$ (37) be imitated (replaced) by an additional Gaussian factor $\exp[-(\alpha_1+\alpha_2)^2/8\pi^2]$, which reduces the azimuthal wave function to the standard double-Gaussian form of Ref. [19]:

$$\widetilde{\Psi} = N \exp\left(-\frac{(\alpha_1+\alpha_2)^2}{2a^2}\right)\exp\left(-\frac{(\alpha_1-\alpha_2)^2}{2b^2}\right) \tag{40}$$

with $N = \sqrt{2/\pi ab}, a = 2\pi, b = \Delta\theta_p/\theta_0$, and, evidently, $a \gg b$. For such wave functions their Schmidt decomposition and Schmidt modes are known [15,16,20]:

$$\widetilde{\Psi}(\alpha_1,\alpha_2) = \sum_n \sqrt{\lambda_n}\psi_n(\alpha_1)\psi_n(\alpha_2), \tag{41}$$

where

$$\lambda_n = \frac{4ab}{(a+b)^2}\left(\frac{a-b}{a+b}\right)^{2n}, \tag{42}$$

ψ_n are Schmidt modes

$$\psi_n = \left(\frac{2}{ab}\right)^{1/4} u_n\left(\frac{\sqrt{2}\,\alpha}{\sqrt{ab}}\right), \tag{43}$$

and $u_n(x)$ are the Hermite-Gaussian functions

$$u_n(x) = (2^n n!\sqrt{\pi})^{-1/2} e^{-x^2/2} H_n(x). \tag{44}$$

The constants λ_n (42) determine the Schmidt parameter K characterizing both the degree of entanglement and the effective dimensionality of the Hilbert space:

$$K = \frac{1}{\sum_n \lambda_n^2} = \frac{a^2+b^2}{2ab} \approx \frac{a}{2b} = \frac{\pi\theta_0}{\Delta\theta_p} = \frac{\pi^2\theta_0\, w}{\lambda_p}. \tag{45}$$

Comparison with Eq. (39) shows that the entanglement parameters K and R are identically equal to each other and, thus, the derivation in terms of Schmidt modes confirms perfectly the very high level of azimuthal entanglement found above.

C. OAM analysis

Let us consider only the azimuthal part (31) of the biphoton angular wave function in the NWO approximation, $\exp[-(\alpha_1-\alpha_2)^2/2[\Delta\alpha^{(c)}]^2]$, with $\Delta\alpha^{(c)} = \theta_0/\Delta\theta_p = \theta_0\lambda_p/\pi w_p$. This function can be expanded in a series of products of adjoint OAM eigenfunctions $e^{il\alpha_1}$ and $e^{-il\alpha_2}$, where $l = 0, \pm 1, \pm 2, \ldots$ are the OAM eigenvalues:

$$\Psi^{\rm az}_{\rm NWO} \propto \sum_l C_l\, e^{il\alpha_1} \times e^{-l\alpha_2}. \tag{46}$$

The expansion coefficients C_l can be easily found to be proportional to $\exp[-l^2[\Delta\alpha^{(c)}]^2/2]$ with $\Delta\alpha^{(c)}$ being the coincidence width of the first Eq. (38). As these coefficients are even in l, only the real part of the product of OAM eigenfunctions gives nonzero contribution into the sum over l; i.e., one can substitute the expression

$$e^{il\alpha_1} \times e^{-il\alpha_2} \equiv \cos[l(\alpha_1-\alpha_2)] + i\sin[l(\alpha_1-\alpha_2)]$$

with

$$\cos[l(\alpha_1-\alpha_2)] = \cos l\alpha_1 \cos l\alpha_2 + \sin l\alpha_1 \sin l\alpha_2.$$

As a result, the normalized azimuthal wave function takes the form of the OAM Schmidt decomposition

$$\Psi(\alpha_1,\alpha_2) = \sum_l \sqrt{\lambda_l^{\rm (OAM)}}\left[\psi^{\rm (cos)}_{l\,\rm OAM}(\alpha_1)\psi^{\rm (cos)}_{l\,\rm OAM}(\alpha_2) + \psi^{\rm (sin)}_{l\,\rm OAM}(\alpha_1)\psi^{\rm (sin)}_{l\,\rm OAM}(\alpha_2)\right], \tag{47}$$

where

$$\lambda_l^{\rm (OAM)} = \frac{\Delta\alpha^{(c)}}{2\sqrt{\pi}}\exp(-l^2[\Delta\alpha^{(c)}]^2), \tag{48}$$

and the OAM Schmidt modes are given by

$$\psi^{\rm (cos)}_{l\,\rm OAM}(\alpha) = \sqrt{\frac{2}{\pi}}\cos l\alpha, \quad \psi^{\rm (sin)}_{l\,\rm OAM}(\alpha) = \sqrt{\frac{2}{\pi}}\sin l\alpha \tag{49}$$

with $|\alpha| \leqslant \pi/2$.

All OAM Schmidt modes are twice degenerate, owing to which the normalization has the form $2\sum_l \lambda_l^{\rm (OAM)} = 1$, which is checked by means of summation substituted by integration over l. The OAM Schmidt entanglement parameter is defined

as the inverse double sum of squared $\lambda_l^{(\mathrm{OAM})}$:

$$K_{az}^{(\mathrm{OAM})} = \frac{1}{2\sum_l \left(\lambda_l^{(\mathrm{OAM})}\right)^2} = \frac{(2\pi)^{3/2}\theta_0 w}{\lambda_p}. \tag{50}$$

Compared to the above-found parameters K (45) and R (39), the OAM Schmidt parameter (50) is about 1.5 times larger, whereas all functional dependencies and estimates by the orders of magnitude in all three cases perfectly coincide. As a whole, this confirms the main conclusion that the azimuthal degree of freedom is rather peculiar compared to all other ones and that, typically, the degree of azimuthal entanglement is very high.

IV. MULTICHANNEL SCHIMDT-TYPE DECOMPOSITION

Thus, the consideration given above indicates that the resource of entanglement that can be accumulated in the azimuthal variables of noncollinear biphotons can be very high. This means that the effective dimensionality of the Hilbert space and the amount of equally important Schmidt modes in any kind of Schmidt decomposition are also very high, on the order of $K_{\mathrm{az}} \sim K_{\mathrm{az}}^{(\mathrm{OAM})} \sim \theta_0 w_p/\lambda_p \sim 10^4$. Such a high amount of important Schmidt modes can make problematic their physical separation, which can be needed for practical purposes. Indeed, the high-order Hermit-Gaussian functions (44) are very strongly oscillating, and neighboring Schmidt modes are very similar to each other. For these reasons, the task of separation of true Schmidt modes in experiments looks almost hopeless. Solution of this problem consists of separation of other orthogonal sub-states, which are not true Schmidt modes, but a superposition of which looks like the Schmidt-type decomposition. A scheme of such an experiment is shown in Fig. 5. In this scheme pairs of photons are collected from a series of different planes (x_n,z) with axes $0x_n \in (xy)$ directed at angles $\alpha^{(n)}$ with respect to the horizontal x axis. In each plane (x_n,z) photons arise approximately at opposite ends of the corresponding diameters around azimuthal angles $\alpha_1^{(n)} = \alpha^{(n)}$ and $\alpha_2^{(n)} = \alpha^{(n)} + \pi$. Black spots at the ends of diameters symbolize receiving fibers, sizes of which are assumed to be larger than the ring thickness ($\sim \Delta\theta_L/\theta_0$) to collect all photons with different polar angles θ at any given α_n. On the other hand, the azimuthal-angle distances between neighboring planes $\alpha^{(n+1)} - \alpha^{(n)}$ must be larger than sizes of receiving fibers and than the coincidence azimuthal width $\Delta\theta_p/\theta_0$. This last condition provides orthogonality of states arising in different planes (x_n,z). After collection, each pair of photons from each given plane (x_n,z) is sent (with equalized optical path lengths) to its own beam splitter, which is a Hong-Ou-Mandel transformer [21] directing united unsplit pairs of photons either to the up or down channels. In this way one can get a multichannel Schmidt-type decomposition with unified pairs of photons originating from each plane (x_n,z) propagating in one of the channels.

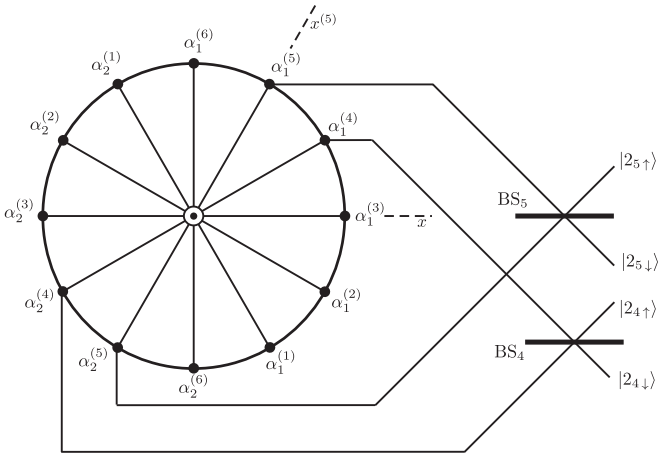

FIG. 5. A scheme of a possible experiment for getting the multichannel Schmidt-type decomposition of noncollinear biphoton states, revealing partially their high resource of azimuthal entanglement; "BS" are beam splitters.

Note that a scheme with collecting photons from different points of the emission ring has been realized experimentally in the works [22,23]. Compared to these experiments, the scheme of Fig. 5 is simpler. In particular, the experiment [22] deals with the four-mode biphoton states, whereas the scheme of Fig. 5 assumes using only two-mode states. Also, a scheme of manipulations with collected photons in the experiment [22] is more complicated than that of Fig. 5, where only a single beam splitter is assumed to be used for any given two-mode state. But the final goals are similar: formation of multipath entangled states. Also, it is worth noting that there are other schemes for creating multichannel orthogonal decompositions, even from a single-plane collection of noncollinear biphotons sent afterwards on the multislit devices [24–26].

By returning to the scheme of Fig. 5, the state vector of all manifold of photons to be collected in the N planes is given by

$$|\Psi\rangle = \frac{1}{\sqrt{N}} \sum_{n=1}^{N} \left|1_{\alpha_1^{(n)}}, 1_{\alpha_2^{(n)}}\right\rangle. \tag{51}$$

The state vector of the state arising after the HOM transformers is given by

$$|\Psi\rangle_{\mathrm{final}} = \frac{1}{\sqrt{2N}} \sum_{n=1}^{N} (|2_{\uparrow n}\rangle - |2_{\downarrow n}\rangle), \tag{52}$$

where the arrows $\uparrow$ and $\downarrow$ indicate the up and downchannels and n indicates the plane $(x_n z)$ from which pairs of photons arrive at the nth beam splitter BS_n. Two such pairs of channels are shown in Fig. 5. Altogether, the state (52) describes a physically separated multichannel Schmidt-type decomposition. In this state each pair of SPDC photons can appear with equal probability $\lambda_n = 1/2N$ in one and only one (but arbitrar) of the $2N$ channels. The degree of entanglement in such a state grows with the growing amount of channels. The Schmidt parameter K and entropy of the reduced density matrix are equal to

$$K = 2N, \quad S_r = -2\sum_{n=1}^{N} \lambda_n \log_2 \lambda_n = 1 + \log_2 N. \tag{53}$$

The maximal amount of channels which can be created in this way is limited by the condition of orthogonality of "modes" arising in neighboring planes, $\alpha^{n+1} - \alpha^n \gg \Delta\alpha^{(c)}$,

where $\Delta\alpha^{(c)} = \pi\theta_0\lambda_p/w_p \sim 10^{-4}$. If $\alpha^{n+1} - \alpha^n$ is taken to be 10 times larger than $\Delta\alpha^{(c)}$, this gives $N_{\max} \sim K_{\max} \sim 10^3$. Of course, in reality the maximal achievable degree of entanglement can be limited at lower values because of technical reasons. Nevertheless, it seems evident that the realizable amount of channels and achievable degree of entanglement in this scheme can be very high.

In principle, with the help of attenuators, the decomposition coefficients in $|\Psi\rangle_{\text{final}}$ (52) can by made different. Also, phases in front of terms $|2_{\uparrow n}\rangle$ and $|2_{\downarrow n}\rangle$ can be arbitrary modified to reduce the state (52) to the form

$$|\widetilde{\Psi}\rangle = \frac{1}{\sqrt{\sum_n(\lambda_{\uparrow n} + \lambda_{\downarrow n})}} \times \sum_{n=1}^{N}(\sqrt{\lambda_{\uparrow n}}e^{i\phi_{\uparrow n}}\,|2_{\uparrow n}\rangle - \sqrt{\lambda_{\downarrow n}}e^{i\phi_{\downarrow n}}\,|2_{\downarrow n}\rangle). \quad (54)$$

With the normalization taken into account and with exclusion of the unmeasurable common phase, this leaves $2(2N-1)$ parameters λ_i and ϕ_i, which can be used for encoding and transmission of information. Being transmitted, this information is readable with a series of measurements. The constants λ_i can be measured by counting numbers of photons in all channels. As for measurement of the phases ϕ_i, one can apply the procedures described in Refs. [11,27]. At first, one has to change photon polarizations ($H \to V$) in one of the channels i_0. Then the signal from this channel has to be merged with the signal from any other channel i with the help of the polarization beam splitter. Finally, the arising unified beam has to be split again by the beam splitter turned 45° around the propagation direction, and the coincidence signal between the two arising channels will provide information about the relative phase $\phi_i - \phi_{i_0}$ [27]. Repeated for all i channels, these measurements will permit one to reconstruct all information accumulated in the constants λ_i and ϕ_i.

V. CONCLUSION

Entanglement of noncollinear biphoton states in azimuthal angles of photon wave vectors is considered, and the degree of azimuthal entanglement is found to be extremely high. The degree of azimuthal entanglement is evaluated by three methods: (1) by finding the parameter R given by the ratio of the single-particle to coincidence widths of the angular distributions, (2) via the Schmidt parameter K found for a model double-Gaussian wave function of two azimuthal angles, and (3) in terms of the OAM analysis, in the frame of which the OAM Schmidt modes and decomposition are defined and found, as well as the OAM Schmidt number $K_{\text{az}}^{\text{OAM}}$. All three methods are found to give the same estimate for the degree of entanglement, which is found to be determined by the ratio of the pump waist to its wavelength times the opening angle of the SPDC emission cone, $\theta_0\, w/\lambda_p$. For reasonably chosen values of all parameters the degree of entanglement and the effective dimensionality of the Hilbert space are found to be on the order of $10^4 \gg 1$. A scheme is suggested for this very high resource of azimuthal entanglement to be seen experimentally, at least partially.

ACKNOWLEDGMENT

The work is supported by the Russian Science Foundation under Grant No. 14-02-01338.

[1] P. G. Kwiat *et al.*, Phys. Rev. A **49**, 3209 (1994).
[2] Y. H. Shih and A. V. Sergienko, Phys. Rev. A **50**, 2564 (1994).
[3] Y.-H. Kim and W. P. Grice, Opt. Lett. **30**, 908 (2005).
[4] C. I. Osorio, G. Molina-Terriza, and J. P. Torres, J. Opt. A: Pure Appl. Opt. **11**, 094013 (2009).
[5] B. Jack, A. M. Yao, J. Leach, J. Romero, S. Franke-Arnold, D. G. Ireland, S. M. Barnett, and M. J. Padgett, Phys. Rev. A **81**, 043844 (2010).
[6] F. M. Miatto, H. Di Lorenzo Pires, S. M. Barnett, and M. P. van Exter, Eur. Phys. J. D **66**, 263 (2012).
[7] D. Giovannini, F. M. Miatto, J. Romero, S. M. Barnett, J. P. Woerdam, and M. J. Padgett, New J. Phys. **14**, 073046 (2012).
[8] C. H. Monken, P. H. Souto Ribeiro, and S. Pádua, Phys. Rev. A **57**, 3123 (1998)
[9] C. K. Law and J. H. Eberly, Phys. Rev. Lett. **92**, 127903 (2004).
[10] M. V. Fedorov, M. A. Efremov, P. A. Volkov, E. V. Moreva, S. S. Straupe, and S. P. Kulik, Phys. Rev. Lett. **99**, 063901 (2007); Phys. Rev. A **77**, 032336 (2008).
[11] M. V. Fedorov, Phys. Scr. **90**, 074048 (2015).
[12] V. G. Dmitriev, G. G. Gurzadyan, and D. N. Nikogosyan, *Handbook of Nonlinear Crystals* (Springer, Berlin, 1997).
[13] D. A. Kalashnikov, M. V. Fedorov, and L. A. Krivitsky, Phys. Rev. A **87**, 013803 (2013).
[14] C. C. Davis, *Lasers and Electro-optics*, 2nd ed. (Cambridge University Press, Cambridge, UK, 2014), Chap. 18, Eq. (18.58).
[15] A. B. U'Ren, K. Banaszek, and I. A. Walmsley, Quant. Inf. Comput. **3**, 480 (2003).
[16] M. V. Fedorov, Yu. M. Mikhailova, and P. A. Volkov, J. Phys. B: At. Mol. Opt. Phys. **42**, 175503 (2009).
[17] P. Kolenderski, W. Wasilewski, and K. Banaszek, Phys. Rev. A **80**, 013811 (2009).
[18] M. V. Fedorov, M. A. Efremov, A. E. Kazakov, K. W. Chan, C. K. Law, and J. H. Eberly, Phys. Rev. A **69**, 052117 (2004).
[19] M. V. Fedorov, M. A. Efremov, P. A. Volkov, and J. H. Eberly, J. Phys. B: At. Mol. Opt. Phys. **39**, S467 (2006).
[20] M. V. Fedorov and N. I. Miklin, Contemp. Phys. **55**, 94 (2014).
[21] C. K. Hong, Z. Y. Ou, and L. Mandel, Phys. Rev. Lett. **59**, 2044 (1987).
[22] A. Rossi, G. Vallone, A. Chiuri, F. De Martini, and P. Mataloni, Phys. Rev. Lett. **102**, 153902 (2009).
[23] G. Vallone, R. Ceccarelli, F. De Martini, and P. Mataloni, Phys. Rev. A **79**, 030301 (2009).

[24] L. Neves, S. Pádua, and C. Saavedra, Phys. Rev. A **69**, 042305 (2004).

[25] L. Neves, G. Lima, J. G. Aguirre Gómez, C. H. Monken, C. Saavedra, and S. Pádua, Phys. Rev. Lett. **94**, 100501 (2005).

[26] L. Neves, G. Lima, E. J. S. Fonseca, L. Davidovich, and S. Pádua, Phys. Rev. A **76**, 032314 (2007).

[27] M. V. Chekhova and M. V. Fedorov, J. Phys. B: At. Mol. Opt. Phys. **46**, 095502 (2013).